Video Article

Quantification of Atherosclerosis in Mice

Monica Centa[1], Daniel F.J. Ketelhuth[1,2], Stephen Malin[1], Anton Gisterå[1]

[1]Cardiovascular Medicine Unit, Center for Molecular Medicine, Department of Medicine, Karolinska Institutet, Karolinska University Hospital

[2]Department of Cardiovascular and Renal Research, Institute for Molecular Medicine, University of Southern Denmark (SDU)

Correspondence to: Anton Gisterå at anton.gistera@ki.se

URL: https://www.jove.com/video/59828
DOI: doi:10.3791/59828

Keywords: Immunology and Infection, Issue 148, Atherosclerosis, ApoE Knockout Mice, Ldlr Knockout Mice, Aorta, Dissection, Microtomy, Staining, Oil red O, Sudan IV

Date Published: 6/12/2019

Citation: Centa, M., Ketelhuth, D.F., Malin, S., Gisterå, A. Quantification of Atherosclerosis in Mice. *J. Vis. Exp.* (148), e59828, doi:10.3791/59828 (2019).

Abstract

Cardiovascular disease is the main cause of death in the world. The underlying cause in most cases is atherosclerosis, which is in part a chronic inflammatory disease. Experimental atherosclerosis studies have elucidated the role of cholesterol and inflammation in the disease process. This has led to successful clinical trials with pharmaceutical agents that reduce clinical manifestations of atherosclerosis. Careful and well-controlled experiments in mouse models of the disease could further elucidate the pathogenesis of the disease, which is not fully understood. Standardized lesion analysis is important to reduce experimental variability and increase reproducibility. Determining lesion size in aortic root, aortic arch, and brachiocephalic artery are common endpoints in experimental atherosclerosis. This protocol provides a technical description for evaluation of atherosclerosis at all these sites in a single mouse. The protocol is particularly useful when material is limited, as is frequently the case when genetically modified animals are being characterized.

Video Link

The video component of this article can be found at https://www.jove.com/video/59828/

Introduction

Cardiovascular disease is the main cause of death in the world with ischemic heart disease and stroke accounting for one in every four deaths[1]. Most cases are caused by atherosclerosis, a disease characterized by a slow build-up of lipid-laden plaques with signs of chronic inflammation in large- and medium-sized arteries[2]. The disease usually remains unnoticed over several decades until a rupture or erosion of the plaque elicits an arterial thrombosis that leads to ischemic tissue damage.

A normal artery consists of an intima layer with endothelial cells and sparsely distributed smooth muscle cells, a media layer with smooth muscle cells and elastic lamellae, and a surrounding adventitial layer with loose connective tissue[3]. An intimal retention of LDL offsets atherosclerosis development[4]. Accumulation and modification of lipoproteins lead to aggregation and entrapment within the arterial intima[5]. An inflammatory response is evoked by the trapped and modified lipoproteins[6]. Endothelial cells start to express adhesion molecules, such as VCAM-1 at sites in the arterial tree with turbulent blood flow, leading to recruitment of circulating monocytes and other leukocytes[7]. The infiltrating monocytes differentiate into macrophages that engulf lipid with ensuing transformation to macrophage foam cells[8].

Atherosclerosis has been studied in mouse models with increasing frequency since the mid-1980s. C57BL/6 is the most commonly used inbred mouse strain for these studies, and it is used as the genetic background for the majority of genetically modified strains[9]. This strain was established in the 1920's[10], and its genome was published in 2002[11]. Experiments in mouse models have several benefits: the colonies reproduce fast, housing is space-efficient, and inbreeding reduces experimental variability. The model also allows for genetic manipulations, such as targeted gene deletions and insertion of transgenes. This has led to new pathophysiological understanding of the disease and new therapy targets[12].

Wild-type C57BL/6 mice are naturally resistant to atherosclerosis. They have most of the circulating cholesterol in HDL, and complex atherosclerotic lesions are not formed even when fed a high-fat and high-cholesterol diet[13]. Hypercholesterolemic mice, such as *Apoe*$^{-/-}$ on the C57BL/6-background, are therefore used as experimental models of atherosclerosis[14,15]. The lack of ApoE impairs hepatic uptake of remnant lipoproteins and severely perturbs lipid metabolism. In *Apoe*$^{-/-}$ mice, circulating cholesterol is predominantly in VLDL particles, and the mice develop complex atherosclerotic plaques on a regular chow diet.

Ldlr$^{-/-}$ mice mimic the development of atherosclerosis seen in humans with familial hypercholesterolemia[16]. The *Ldlr*$^{-/-}$ mice need a Western type diet to develop atherosclerosis[17]. Western diet mimics human food intake and usually contains 0.15% cholesterol. The LDL receptor recognizes ApoB100 and ApoE and mediates uptake of LDL particles through endocytosis. LDL receptors are fundamental for liver clearance of LDL from circulation, while LDL receptor expression in hematopoietic cells does not influence this process. This opens the possibility for bone marrow transplantation of *Ldlr*$^{+/+}$ cells into hypercholesterolemic *Ldlr*$^{-/-}$ recipients and assessment of atherosclerosis development. Bone marrow

chimeras have commonly been used to study the participation of hematopoietic cells in experimental atherosclerosis. However, bone marrow transplantation could influence the size and composition of atherosclerotic plaques, making interpretation of results ambiguous.

Different variants of *Apoe*$^{-/-}$ and *Ldlr*$^{-/-}$ mice with additional genetic alterations have been developed to study specific processes of the disease[18]. One example is human *APOB100*-transgenic *Ldlr*$^{-/-}$ (*HuBL*) mice that carry the full-length human *APOB100* gene[19,20]. These mice develop hypercholesterolemia and atherosclerosis on a regular chow diet. However, the development of complex atherosclerotic plaques takes at least six months and shorter experimental protocols usually use Western diet[21]. A large fraction of plasma cholesterol is circulating in LDL particles, which gives *HuBL* mice a more human-like dyslipidemic lipoprotein profile compared to *Apoe*$^{-/-}$ and *Ldlr*$^{-/-}$ mice. *HuBL* mice also allow studies of human apoB as an autoantigen[22].

The mouse models of atherosclerosis develop complex atherosclerotic plaques with shared features of human disease. However, the plaques are fairly resistant to rupture with ensuing myocardial infarction. Atherothrombosis is only sporadically detected and experimentally challenging to assess[23,24,25]. Special models of plaque rupture have been developed, but the experimental field lacks a reliable and reproducible model for assessment of plaque stabilizing agents.

Quantification of atherosclerosis has been reported in numerous ways in the literature. Recent efforts have tried to standardize experimental design, execution, and reporting of animal studies[26]. Investigators have different preferences and techniques adapted to their laboratories. Most research projects are also unique in a way that they require some protocol modifications. Due to the multifactorial nature of the disease, optimal controls vary between projects. Local conditions and lack of standardization may cause observed differences in disease development, which hampers advances of the research field. Differences in experimental variability also means that statistical power calculations need to be based on pilot studies under local conditions.

Quantification of atherosclerosis is recommended at several locations in the vascular tree. This protocol describes how to obtain results from the aortic root, the aortic arch, and the brachiocephalic artery in a single mouse, in addition to leaving the rest of the thoracoabdominal aorta for other analyses. En face preparations allow rapid quantification of lipid-laden plaques in the aortic arch. Disease burden in the brachiocephalic artery can also be quantified if the specimens are carefully displayed. The more time consuming cross-sectioning of the aortic root leaves several sections available for detailed evaluation of plaque composition.

Protocol

All animal experiments require approval by ethical authorities.

1. Mouse Sacrifice and Microdissection of Aorta

1. Sacrifice the mouse by CO_2 asphyxiation and record weight.
2. Spray the mouse with 70% ethanol to avoid fur contamination of the samples. Place the mouse in a supine position. From the jugular notch, make a midline incision using Mayo scissors extending it almost down to the pubic bone.
   CAUTION: High percentage ethanol is highly flammable and could cause serious eye irritation. Take precautionary measures.
3. Use a 23 G needle to exsanguinate the mouse by cardiac puncture through the thorax wall. This procedure usually yields 750 µL of blood from a 20 week old mouse. Typically, collect half of the volume in a tri-potassium EDTA-coated tube and the other half in a serum or lithium heparin-coated tube. Gently turn the tubes and keep them at room temperature until further processing.
4. **Use Mayo scissors to cut the parietal peritoneum in the midline to open the abdominal cavity. Hold the xiphoid process with tissue forceps and cut open the peritoneum laterally on both sides and continue to open the diaphragm.**
   1. Use the Mayo scissors to open the chest cavity by cutting through the rib cage as laterally as possible. This will enable wide angles for the instruments while microdissecting the aorta later on.
5. Make an incision in the right auricle for perfusion fluid drainage. Insert a 27 G needle through the apex of the heart in cranial direction. Keep the needle fixed in the left ventricle while slowly perfusing the mouse with 10 mL ice-cold phosphate-buffered saline (PBS) during minimum 2 min. Observe the liver shifting in color and getting paler.
   NOTE: Some protocols use paraformaldehyde perfusion, but this interferes with several downstream applications, such as immunohistochemistry analysis of lymphocytes. Therefore, no perfusion fixation with paraformaldehyde is performed in this protocol.
6. Dissect organs of interest (e.g. lymph nodes, spleen, liver, intestine, inguinal fat pads, kidneys, etc.) using anatomical forceps and dissecting scissors.
7. Cut trachea and esophagus on the right side of the heart without damaging the aortic arch. Cut the diaphragm and structures attaching the viscera to retroperitoneum, leaving the heart, aorta, and kidneys in situ. Fold away the lungs and viscera caudally and cover them with a napkin to begin retroperitoneal microdissection of para-aortic lymph nodes and abdominal aorta.
8. **Start microdissection under a stereomicroscope at 6x magnification. Begin to dissect the aortic bifurcation by lifting surrounding tissue with Dumont forceps and cutting under tension with Vannas scissors.**
   1. Continue dissection of the abdominal aorta cranially. Cut abdominal branches from the aorta and free the aorta proximally through the aortic hiatus in the diaphragm.
      NOTE: Microdissection requires accurate hand-eye coordination through the stereomicroscope, which takes some practice to master.
9. Remove the adipose tissue covering the thoracic aorta. Carefully dissect dorsally of the thymus to free the aortic arch with branches. Continue dissecting the carotid arteries as distally as possible in the thoracic cavity. In special cases, neck dissection could be performed to include the carotid bifurcation.
10. Clean the instruments by consecutive rinses in deionized water, RNase decontamination solution, 70% ethanol, and PBS before actually cutting the aorta. Lift the heart by the apex with the forceps. Cut the aorta close to the heart and place the whole heart in a tube with PBS. The heart could be stored on ice for a couple of hours before continued processing and cryomounting the aortic root.

11. Cut the aortic arch according to **Figure 1A**. Put the aortic arch in a tube containing 1 mL of 4% formaldehyde overnight at 4 °C. The specimen could be stored in this manner for several years before pinning and analysis.
CAUTION: Formaldehyde may cause cancer, allergic skin reactions, and is harmful if swallowed. Use personal protective equipment as required.
12. Dissect the remaining descending aorta and put it in an RNA stabilization solution or snap freeze it for subsequent RNA analysis or other application. Optimizing work flow to minimize dissection time is crucial to avoid excessive RNA degradation.
13. Put the blood collection tubes (collected in step 1.3) in a centrifuge. Spin down the separate plasma and serum tubes at 1,500 x *g* for 15 min at room temperature. Carefully transfer the plasma and serum to microcentrifuge tubes and store at -80 °C. Collecting both EDTA and heparinized plasma or serum leaves possibilities for multiple downstream applications.
14. **Place the heart on a cork bed with the ventral side facing up. Fix the heart to the cork with a needle through the apex. Hold the base of the heart with anatomical forceps.**
    1. Use a scalpel to cut away the apical 2/3 of the heart with the direction of the cut being as a line between the two auricles with the scalpel angled 20° caudally in the sagittal plane and 20° cranially in the transversal plane (**Figure 1B**).
15. Embed the aortic root in optimum cutting temperature (OCT) compound, which surrounds, but do not infiltrate the tissue. Immerse the base of the heart in OCT compound. Gently squeeze the heart with the forceps to fill the aortic root with OCT and remove any air bubbles.
16. Transfer the specimen to the bottom of a cryomold filled with OCT. The aortic root should now be perpendicular to the bottom surface. Put the mounted heart on dry ice to freeze. Store the specimens in zip lock bags in -80 °C until pursuing cryosectioning according to section 3 in this protocol.

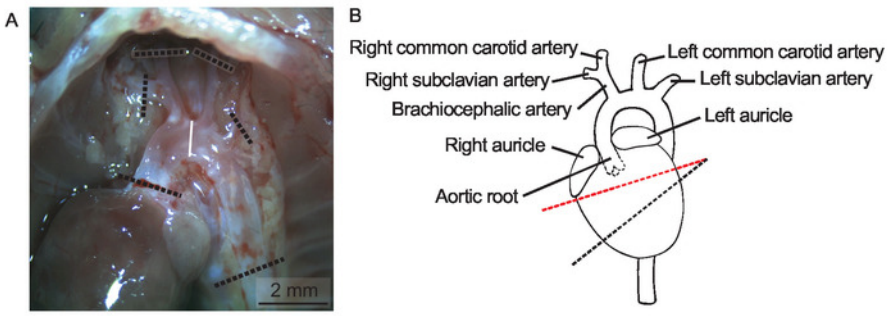

Figure 1: Heart and aortic arch in situ. (**A**) Lungs, trachea, esophagus, and thymus are removed to display the aortic arch in situ in a 20 weeks old female *Apoe*$^{-/-}$ mouse on regular chow diet in a micrograph, Scale bar = 2 mm. The dotted lines indicate where to cut the aortic arch and its branches. (**B**) A schematic depiction of the heart and aorta. The dotted line in red indicates where to cut the heart before cryomounting the aortic root. Please click here to view a larger version of this figure.

2. En Face Analysis of Aortic Arch and Brachiocephalic Artery

1. Prepare pinning beds for en face analysis of aortic arches. Fold a segment of paraffin wax film eight times to make a flat 25 mm x 25 mm surface. Wrap it with black electric insulation tape to make a dark background for the aorta. Place a label on the backside of the pinning bed and use a lead pencil to write the mouse identification number (normal pen ink will disappear in the staining process).
2. **Transfer the aortic arch to the pinning bed and place a drop of PBS on top of it. Begin cleaning the aorta from remaining periadventitial adipose tissue under a stereomicroscope.**
    1. Use Vannas scissors and Dumont forceps to gently peel away all surrounding adipose tissue without manipulating or damaging the aorta. The Sudan IV will stain adipose tissue brightly and it is crucial to remove all such tissue at this point.
    NOTE: Keep the aorta moist at all times applying additional PBS when needed.
3. **Cut open the aorta in the coronal plane by introducing the Vannas scissors in the aortic lumen to expose the intimal surface. Begin to cut the outer curvature of the ascending arch in distal direction and continue to cut open the branches including the brachiocephalic artery. Spare the dorsal part of the descending thoracic region.**
    1. Cut open the lesser curvature and fold open the aorta to display the intimal surface.
    NOTE: This step requires fine motor skills and needs some practice to master.
4. Pin the open arch to the pinning bed using the blunt end of minutien insect pins. Use a micro Castroviejo needle holder to put the pins in place. Gently bend the pins away from the specimen when in place. Pin the aorta flat on the bed without stretching the specimen. Store the pinned arch facing downwards in a Petri dish filled with PBS at 4 °C.
NOTE: The protocol can be paused here.
5. Prepare a working solution of Sudan IV. Mix 1 g of Sudan IV powder, 100 mL of 70% ethanol, and 100 mL of acetone in a dark bottle and gently stir for 10 min. There is no need to filter the solution and it can be used for a couple of months if kept dark at room temperature. If the staining color is not satisfactory, a new solution can be made and the specimens stained again.
CAUTION: Acetone is a flammable liquid that could cause serious eye irritation. Store in a well-ventilated place and take precautionary measures when handling.
6. **Arrange five Petri dishes on the lab bench: one filled with 70% ethanol, one filled with Sudan IV working solution, two filled with 80% ethanol, and one filled with PBS.**
    1. Start with rinsing the specimen in 70% ethanol for 5 min by placing the pinning bed in the first Petri dish with the arch facing downwards. Transfer the specimen to the Sudan IV working solution and let it stain the arch for 7 min.

2. Next, rinse in 80% ethanol for 3 min twice to destain the normal intimal surface. Destaining time could be adjusted to optimize results. Lastly, rinse in PBS before putting the specimen back into the original Petri dish.

7. Acquire micrographs using a stereomicroscope at 10 times magnification connected to a digital camera. Take pictures of the pinned arch submerged in PBS using small metal weights (20 mm x 10 mm x 5 mm) to hold the pinning bed to the bottom of a Petri dish. Place a ruler next to the aorta for calibration of the image.
8. **Use an image analysis software (e.g. ImageJ) to determine lesion area and total intimal surface. In lack of anatomical landmarks to define the aortic arch, measurement is usually performed from the start of the ascending aorta down to the first intercostal branch (Figure 2A). Use the area quantification feature in the software to manually encircle the total intimal arch area.**
NOTE: The lesion quantification should be done in a blinded fashion and it is advisable that a second investigator confirms the results.
    1. In ImageJ, select the polygon selection tool and encircle the total arch area by repetitive clicks. Then select measure in the analyze menu to display the total arch area in the result window.
    2. Next, encircle all Sudan IV-stained plaques in the arch. Sudan IV is a lysochrome diazo dye that stains lipids, triglycerides, and lipoproteins with an orange-red color. In ImageJ, select the freehand selection tool and encircle all plaques while pressing the Alt key. Click measure in the analyze menu to display lesion-free arch area in the result window.
    3. Calculate relative lesion area by subtracting the lesion-free area from the total arch area and then dividing the result with the total arch area.

9. **Carefully pin the subclavian and carotid arteries to enable lesion quantification in the brachiocephalic artery (Figure 2A). Quantification of lesions in the subclavian arteries and the common carotid arteries is usually very challenging and not meaningful, respectively.**
    1. In ImageJ, encircle both pieces of the braciocephalic artery using the polygon selection tool while pressing the shift key. Click measure in the analyze menu to display the total brachiocephalic artery area in the result window.
    2. Next, select the freehand selection tool and encircle all plaques in brachiocephalic artery while pressing the Alt key. Click measure in the analyze menu to display the lesion-free brachiocephalic artery area in the result window.
    3. Calculate relative lesion area by subtracting the lesion-free area from the total brachiocephalic artery area and then dividing the result with the total brachiocephalic artery area.

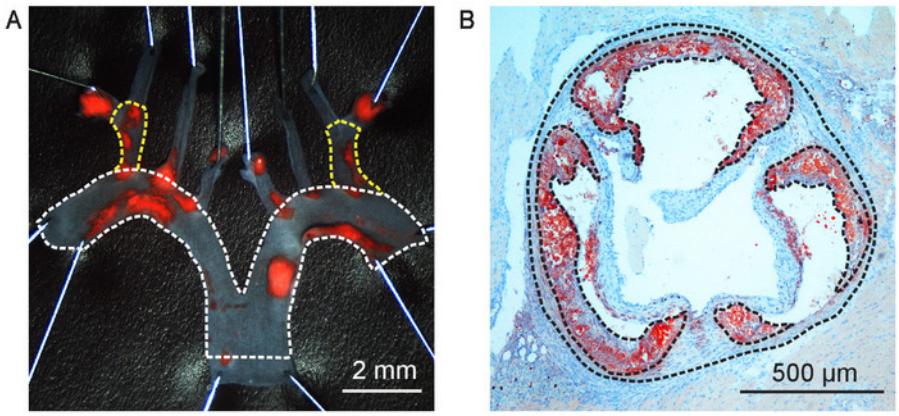

Figure 2: Atherosclerotic lesion quantification. (**A**) Aortic arch from a 20 weeks old male human *APOB100*-transgenic *Ldlr*$^{-/-}$ (*HuBL*) mouse fed Western diet for ten weeks pinned open and stained for lipid-rich plaques with Sudan IV. Total aortic arch surface area is outlined with the dotted line in white in the micrograph, Scale bar = 2 mm. The dotted lines in yellow outline the total surface area of the brachiocephalic artery. (**B**) Aortic root cross-section at 400 µm from the aortic sinus in a 20 weeks old male *Ldlr*$^{-/-}$ mouse fed Western diet for eight weeks visualized in a micrograph, Scale Bar = 500 µm. The dotted lines in black outline the total vessel area and atherosclerotic lesions stained with Oil Red O localized in the arterial intima. Please click here to view a larger version of this figure.

3. Cryosectioning of the Aortic Root

1. Set the cryostat temperature at -20 °C and section thickness to 10 µm. Mount the OCT block containing the aortic root on the specimen holder with the ventricular tissue facing outward. While starting to cut, fine tune the alignment of the section surface to be parallel to the specimen holder.
2. Remove excessive surrounding OCT to make it easier to collect sections without folds. The aortic root should now be positioned perpendicular to the knife blade given that the base of the heart was placed correctly in the mold.
3. Collect initial control sections on ordinary microscope slides, which will be discarded. The first sections should only contain heart muscle tissue. Progress the sectioning by 200 µm at the time. Collect a section and check the progress with a light microscope.
4. When getting closer to the left ventricle outflow tract, check every 100 µm under the microscope. When initial indications of a vessel wall are observed, slow down the pace to 50 µm.
NOTE: When the first aortic cusp appears, this will be point zero for collecting sections. It can be difficult to see when the cusps appear exactly, but an exact localization is crucial to perform comparisons of lesions in the same region.
5. **Tilt the specimen towards the point zero cusp to align the section plane with the two other cusps. This is crucial for obtaining true cross sections of the aorta. Make a drawing of the aortic root, indicating the cusps as they appear, and count every 10 µm section that are cut from point zero onwards.**

1. When a second cusp appears, slightly tilt the specimen again away from the cusp to align the specimen with the third cusp. The level difference between the cusps should not exceed 50 µm. Start to collect sections on slides from level 90 µm and onwards.
2. Collect sections according to the slide planning in **Figure 3**. The collection of sections may be started from 190 µm if the aortic root is more than 50 µm tilted, to allow further space to align the root in a straight position. Continue sectioning until reaching level 800 µm from point zero. If there are still visible plaques at this level, the collection could be expanded to 1,000 µm.
NOTE: A simplified slide organization is presented in **Supplemental Figure 1**, which could increase sectioning speed. The optimal slide planning should be decided depending on the project plan.

6. **Fix the sections after collection.**
1. Fix the sections collected for Oil Red O staining and Picrosirius red staining of collagen in 4% formaldehyde for 10 min. Rinse in deionized water, dry, and store in room temperature until pursuing with section 4 in this protocol. If slides should be stained with Oil Red O right away and are still wet, place them in 60% isopropanol for 1 min to speed up the drying process.
CAUTION: Isopropanol is a flammable liquid that could cause serious eye irritation and may cause drowsiness or dizziness. Store in a well-ventilated place and take precautionary measures when handling.
2. Fixate the sections collected for immunohistochemistry or immunofluorescence in ice cold pure acetone for 10 min. Dry in room temperature for 30 min. Store sections in -20 °C.

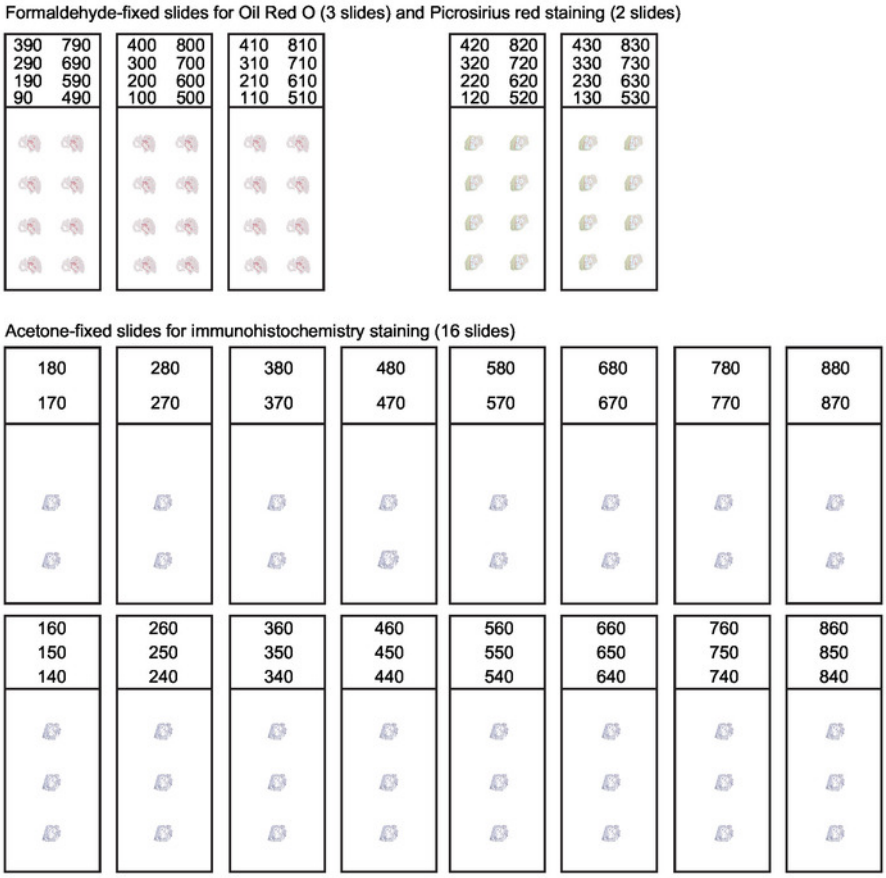

Figure 3: Organization of slides for serial sections of the aortic root. During cryosectioning of the aortic root every 10 µm thick section spanning the first 800 µm of the ascending aorta should be collected. A systematic slide organization is needed to obtain suitable sections for various applications. Analysis of lesion composition usually includes Oil Red O staining for lipids and Picrosirius red staining for collagen. Remaining sections are collected and acetone-fixed for immunohistochemistry and immunofluorescence staining. This figure has been modified from Gisterå et al[30]. Please click here to view a larger version of this figure.

4. Oil Red O Staining and Quantification of Atherosclerosis in Aortic Roots

1. Prepare a saturated Oil Red O solution by dissolving 1 g of Oil Red O in 100 mL of isopropanol. Stir the solution in a dark bottle for 1 hour at room temperature. The saturated solution can be kept for several months.
NOTE: It is advisable to have designated laboratory equipment for Oil Red O staining since it is difficult to clean equipment that has been in contact with the solution.
2. Prepare a working solution by mixing 75 mL of the saturated Oil Red O solution with 50 mL of deionized water. Let stand in room temperature for 10 min. Filter through a qualitative filter paper.
3. Place the slides in Oil Red O working solution for 20 min. Rinse in tap water for 5 min.
4. To assist tissue visualization, stain with Mayer's hematoxylin for 1 min. Rinse in lukewarm tap water for 5 min. All nuclei should now be stained in blue color, adjust staining time to optimize the result.

5. Mount slides in an aqueous mounting medium (e.g., Kaiser's glycerol gelatin). Warm Kaiser's glycerol gelatin to 40 °C to make it fluid before use. It is not necessary to dry the slides since the mounting medium is water based. Be careful to avoid air bubble formation when adding the cover glass.
   CAUTION: Kaiser's glycerol gelatin contains phenol, which is suspected of causing genetic defects. Use personal protective equipment as required.
6. Acquire digital micrographs using a camera connected to a light microscope. Usually the full vessel wall and lesion boundaries could be clearly visualized by 50 times magnification. Save high resolution images, preferably in tagged image file format (TIFF).
7. **Perform analysis of lesion size using a computer-assisted image analysis software system. Oil Red O is a lysochrome diazo dye that stains neutral lipids and visualizes atherosclerotic plaques with an intense red color, which assists lesion quantification.**
   NOTE: The lesion quantification should be done in a blinded fashion and it is advisable that a second investigator confirms the obtained results.
   1. Use the area quantification feature in the image analysis software to define the total vessel area by encircling the external elastic lamina of the aortic vessel wall (**Figure 2B**). In ImageJ, select the polygon selection tool and encircle the area by repetitive clicks. Then select measure in the analyze menu. The total vessel area is displayed in the result window.
   2. Continue to quantify the atherosclerotic lesions in the intimal layer of the vessel, defined by the internal elastic lamina and the luminal boundary. Usually lesions on valve cusps are excluded from the measurement[27]. In ImageJ, select the freehand selection tool and encircle all plaques while pressing the Alt key. Select measure in the analyze menu to display the lesion-free vessel area in the result window.
   3. Calculate the relative lesion area by subtracting the lesion-free area from the total vessel area and then dividing the result with the total vessel area.
      NOTE: Calibrate the results in the image analysis software according to the used magnification to obtain absolute lesion area in square micrometer.

8. **Define the Oil Red O-stained area in the lesions by using a color threshold feature in the image analysis software to calculate the percentage of Oil Red O positive area of total lesion area.**
   1. In ImageJ, encircle all lesion area by using the freehand selection tool while pressing the shift key. Select measure in the analyze menu to display total lesion area is in the result window.
   2. Select clear outside in the edit menu. Change the image type to 8-bit in the image menu.
   3. Set a red threshold for Oil Red O negative area by selecting threshold in the adjust submenu of the image menu. Click apply. Make the image binary by selecting this option in the binary submenu of the process menu.
      NOTE: Usually Oil Red O staining varies between batches. Hence, color thresholding is only recommended within the same staining batch. The result should be presented along with a description how the threshold was determined and standardized.
   4. Analyze the picture by selecting analyze particles in the analyze menu and click ok. Total Oil Red O negative lesion area is now displayed in the summary window. Calculate the relative Oil Red O positive area by subtracting the Oil Red O negative area from the total lesion area and then dividing with the total lesion area.

Representative Results

In mouse models of atherosclerosis the most prominent lesions tend to develop in the aortic root and aortic arch. This protocol describes quantification of atherosclerosis in the aortic root, the aortic arch, and the brachiocephalic artery in a single mouse. Measurable lesions in thoracic descending aorta and abdominal aorta are only present in animals with advance disease. In this protocol, these parts are not analyzed for atherosclerotic burden, but saved for subsequent analysis of mRNA levels or other analyses. Serial sections of atherosclerotic lesions in the aortic root are usually displayed in a graph with lesion size on the *y*-axis and distance to the aortic sinus on the *x*-axis[28]. True cross-sections are crucial for lesion size quantification. Oblique sections can overestimate lesion sizes and a tilting of only 20° could overestimate the absolute lesion surface by 15%[29]. However, calculating the lesion fraction of total vessel area makes the result less sensitive to possible angle differences during sectioning (**Figure 4A**). An appropriate statistical method to detect differences between groups is usually a regular 2-way analysis of variance (ANOVA). Bonferroni post-tests are then carried out to detect differences at certain levels. Fisher's least significant difference could also be used as a follow-up test to ANOVA. It reduces the likelihood of type II statistical errors, but do not account for multiple comparisons. In addition, it could be illustrative to calculate area under the curve or the average lesion size per mouse and present the data in a dot plot to further visualize individual variation within the groups (**Figure 4B**).

Oil Red O is a fat-soluble bright red diazo dye, which stains neutral lipids. Polar lipids in cell membranes are not stained. Oil Red O staining can be performed on fresh, frozen, or formalin-fixed samples, but not on paraffin-embedded samples due to the removal of lipids in the required deparaffinization process. A quantification of lesional lipid accumulation could be performed by color thresholding the Oil Red O positive area of total lesion area (**Figure 4C**). Hematoxylin produces a blue staining of cell nuclei, which is helpful to visualize plaque morphology. The right and left coronary arteries usually diverge from the aorta around 250 µm from the aortic sinus[27], which often coincide with the most prominent lesion sizes. Cross-sections from this region is often displayed as representative results (**Figure 4D**).

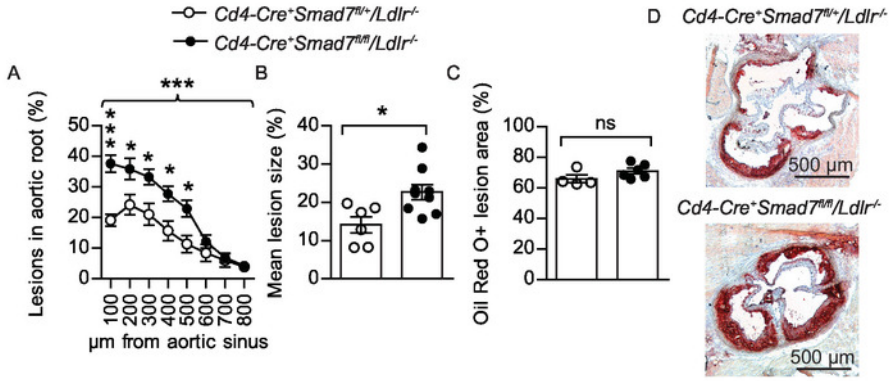

Figure 4: Atherosclerotic lesions in the aortic root. (**A**) Twenty-eight weeks old male bone marrow chimeras fed Western diet for eight weeks were evaluated to determine the effect of *Smad7*-deficient T cells on atherosclerosis development. Experimental *Ldlr*$^{-/-}$ chimeras received *Cd4-Cre*$^{+}$*Smad7*$^{fl/fl}$ bone marrow and controls received *Cd4-Cre*$^{+}$*Smad7*$^{fl/+}$ bone marrow. The graph shows quantification of atherosclerotic lesion area from eight consecutive sections, 100 - 800 µm from the aortic sinus displayed as lesion fraction of total vessel surface (*Cd4-Cre*$^{+}$*Smad7*$^{fl/+}$/*Ldlr*$^{-/-}$ n=6, *Cd4-Cre*$^{+}$*Smad7*$^{fl/fl}$/*Ldlr*$^{-/-}$ n = 9, 2-way ANOVA with Bonferroni's post test, graph shows mean ±SEM, braces indicate significance level for strain comparison). (**B**) The combined dot plot and bar graph shows the mean atherosclerotic lesion area from the aortic root sections (*Cd4-Cre*$^{+}$*Smad7*$^{fl/+}$/*Ldlr*$^{-/-}$ n=6, *Cd4-Cre*$^{+}$*Smad7*$^{fl/fl}$/*Ldlr*$^{-/-}$ n = 9, Student's *t*-test) (**C**) Fraction of Oil Red O-stained area in the lesions (*Cd4-Cre*$^{+}$*Smad7*$^{fl/+}$/*Ldlr*$^{-/-}$ n = 4, *Cd4-Cre*$^{+}$*Smad7*$^{fl/fl}$/*Ldlr*$^{-/-}$ n = 6, Student's *t*-test, ns=non-significant) (**B**-**C**) Dots represent individual mice and bars show mean ±SEM. (**D**) Representative micrographs showing Oil Red O staining (in red color) of neutral lipids in the aortic root 300 µm from aortic sinus (50x magnification), Scale bar = 500 µm. *$p \leq 0.05$, ***$p \leq 0.001$. This figure has been modified from Gisterå et al.[31]. Please click here to view a larger version of this figure.

Oil Red O could be used for staining of en face prepared aortas, but this protocol uses Sudan IV, another convenient fat-soluble diazo dye. Sudan IV clearly visualizes atherosclerotic plaques in an orange-red color by staining lipids, triglycerides, and lipoproteins. Removing the dark background in representative images of the en face aortic arches could enhance the visual display (**Figure 5A**). Usually lesion size is normally distributed within groups, allowing statistical testing with Student's *t*-test between groups. A dot plot that shows both individual mice and the mean, which is compared between groups, is an informative way to display the results (**Figure 5B-C**). Since the variation within groups typically is different between locations in the vascular tree, separate power calculations are usually needed. Unnecessary variation can be avoided by method proficiency and protocol standardization. Obtaining statistically significant results is important, but the biological relevance for an observed difference always needs to be considered as well.

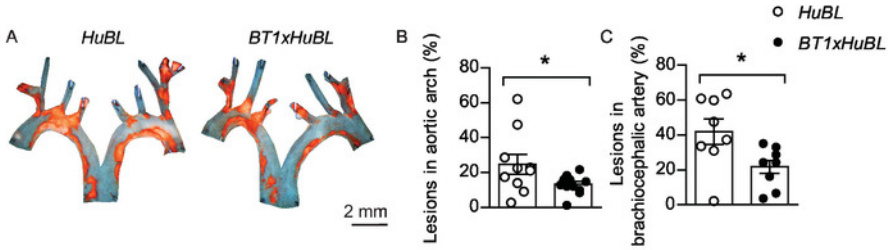

Figure 5: Atherosclerotic lesions in aortic arch and brachiocephalic artery. (**A**) Representative en face micrographs of aortic arches with lipid-laden plaques stained with Sudan IV (in orange color) from 20 weeks old mice fed Western diet for ten weeks, visualized together. Scale bar = 2 mm. Human *APOB100*-transgenic *Ldlr*$^{-/-}$ (*HuBL*) mice were used as controls and the experimental group consisted of TCR-transgenic mice with LDL-reactive T cells (*BT1*) crossbred to *HuBL* mice. (**B**) Atherosclerotic lesions in the aortic arch (*HuBL* n = 10, *BT1xHuBL* n = 12; Student's *t*-test). (**C**) Atherosclerotic lesions in the brachiocephalic artery (*HuBL* n = 8, *BT1xHuBL* n = 9, Student's *t*-test). (**B**-**C**) Dots represent individual mice, bars show mean ±SEM. *$p \leq 0.05$. This figure has been modified from Gisterå et al.[32]. Please click here to view a larger version of this figure.

Supplemental Figure 1: Alternative organization of slides for serial sections of the aortic root. A simplified systematic slide organization for collection of sections from the aortic root. The collection enables Oil Red O staining for lipids and immunohistochemistry or immunofluorescence staining. Dedicated slides for Picrosirius red staining of collagen are omitted. Please click here to download this file.

Discussion

Cardiovascular disease is the main killer in the world and new preventive measurements are needed[2]. Mouse models of the disease provide a comprehensive platform for investigation of pathophysiology and experimental treatments[13]. Reliable lesion size quantification is essential for this approach. However, quantification methods differ between laboratories. Standardization and optimization have been an ongoing process since the 1980's[13,27,33,34]. Aortic roots have emerged as the most popular site to quantify experimental atherosclerosis. Cross-sections of plaques enable comparison of plaque volume between groups. En face preparations are favored for lesion quantification in larger segments of the aorta. The en face method visualizes plaque quantity and enables quantification of plaque area coverage, but do not take plaque thickness in account. The biological relevance for observed differences is substantiated by coherent results at different locations in the vascular tree. Evaluating atherosclerosis development at different locations addresses possible site specific effects. The effect of transplanted hematopoietic cells on atherosclerosis development can be assessed in hypercholesterolemic *Ldlr*$^{-/-}$ chimeras. However, whole-body irradiation affects the

atherosclerosis process with site specific effects. More prominent atherosclerotic lesions are developed in the aortic root, while reduced lesion development is observed in aortic arches[35].

Importantly, not only lesion size needs to be addressed in studies of experimental atherosclerosis. Lesion composition is also a key parameter. Several plaque features have been associated with manifestations of the disease in humans[36]. Serial sectioning of the aortic root leaves several sections available for careful analysis of plaque composition. Plaque rupture in humans is characterized by a thin fibrous cap with few smooth muscle cells, sparse collagen content and signs of inflammation in the plaques[36]. Although plaque rupture is a rare event in mouse models of atherosclerosis, markers for plaque stability are informative to evaluate. Translational approaches could confirm mechanistic findings from mouse models and uncover important features of human disease[31]. Inflammatory status of atherosclerotic plaques could be determined by immunohistochemistry staining of VCAM-1, MHC class II, macrophages, and lymphocytes[30]. Some protocols use longitudinal sections in the coronal plane of the aortic arch or the brachiocephalic artery for measuring atherosclerotic lesion size and composition[37]. However, this alternative method leaves only few sections to be analyzed, which limits its applications.

An initial critical step in this protocol is the ability to harvest aortas efficiently. Hand-eye coordination under the microscope requires practice and is crucial both for the microdissection and the subsequent pinning of the aortic arch. The next critical step in this protocol is the collection of serial sections from the aortic root. Eighty consecutive sections should be collected for each mouse, which requires both focus and patience. Methodological proficiency could speed up the described processes considerably. Nevertheless, atherosclerotic lesion quantification is still a time-consuming task. New technology, automated handling, and small animal imaging might facilitate quantification of experimental atherosclerosis in the future. The progression of atherosclerosis is slow and most experimental protocols in mouse models take more than four months to complete[13]. Therefore, aortas need to be collected in an optimized way at study endpoints. This protocol provides a comprehensive guide to harvest aortas efficiently and the proposed processing prepares aortas for multi-purpose use including lesion quantification in aortic root, aortic arch, and brachiocephalic artery. Hopefully the protocol can reduce experimental variability, enhance reliability of results, and lead to findings that will pave the way for new treatments against atherosclerosis.

Disclosures

The authors have nothing to disclose.

Acknowledgments

We thank all past members of Göran K Hansson's experimental cardiovascular research unit that helped develop this protocol over the past quarter-century. We are particularly grateful for the contributions by Antonino Nicoletti, Xinghua Zhou, Anna-Karin Robertson, and Inger Bodin. This work was supported by project grant 06816 and Linnaeus support 349-2007-8703 from the Swedish Research Council, and by grants from the Swedish Heart-Lung Foundation, Stockholm County Council, Professor Nanna Svartz foundation, Loo and Hans Osterman Foundation for Medical Research, Karolinska Institutet's Research Foundation and Foundation for Geriatric Diseases at Karolinska Institutet.

References

1. Lozano, R. et al. Global and regional mortality from 235 causes of death for 20 age groups in 1990 and 2010: a systematic analysis for the Global Burden of Disease Study 2010. *Lancet.* **380** (9859), 2095-2128 (2012).
2. Gistera, A., Hansson, G. K. The immunology of atherosclerosis. *Nature Reviews Nephrology.* **13** (6), 368-380 (2017).
3. Hansson, G. K. Inflammation, atherosclerosis, and coronary artery disease. *New England Journal of Medicine.* **352** (16), 1685-1695 (2005).
4. Williams, K. J., Tabas, I. The response-to-retention hypothesis of early atherogenesis. *Arteriosclerosis, Thrombosis, and Vascular Biology.* **15** (5), 551-561 (1995).
5. Pentikainen, M. O., Oorni, K., Ala-Korpela, M., Kovanen, P. T. Modified LDL - trigger of atherosclerosis and inflammation in the arterial intima. *Journal of Internal Medicine.* **247** (3), 359-370 (2000).
6. Ruuth, M. et al. Susceptibility of low-density lipoprotein particles to aggregate depends on particle lipidome, is modifiable, and associates with future cardiovascular deaths. *European Heart Journal.* **39** (27), 2562-2573 (2018).
7. Nakashima, Y., Raines, E. W., Plump, A. S., Breslow, J. L., Ross, R. Upregulation of VCAM-1 and ICAM-1 at atherosclerosis-prone sites on the endothelium in the ApoE-deficient mouse. *Arteriosclerosis, Thrombosis, and Vascular Biology.* **18** (5), 842-851 (1998).
8. Goldstein, J. L., Ho, Y. K., Basu, S. K., Brown, M. S. Binding site on macrophages that mediates uptake and degradation of acetylated low density lipoprotein, producing massive cholesterol deposition. *Proceedings of the National Academy of Sciences of the United States of America.* **76** (1), 333-337 (1979).
9. Paigen, B., Morrow, A., Brandon, C., Mitchell, D., Holmes, P. Variation in susceptibility to atherosclerosis among inbred strains of mice. *Atherosclerosis.* **57** (1), 65-73 (1985).
10. Russell, E. S. Origins and history of mouse inbred strains: contributions of Clarence Cook Little. *Origins of Inbred Mice, Morse, HC, eds. (Academic Press, NY).* 33-43 (1978).
11. Waterston, R. H. et al. Initial sequencing and comparative analysis of the mouse genome. *Nature.* **420** (6915), 520-562 (2002).
12. Gistera, A., Ketelhuth, D. F. J. Lipid-driven immunometabolic responses in atherosclerosis. *Current Opinion in Lipidology.* **29** (5), 375-380 (2018).
13. Maganto-Garcia, E., Tarrio, M., Lichtman, A. H. Mouse models of atherosclerosis. *Current Protocols in Immunology.* **Chapter 15** Unit 15.24.11-23 (2012).
14. Plump, A. S. et al. Severe hypercholesterolemia and atherosclerosis in apolipoprotein E-deficient mice created by homologous recombination in ES cells. *Cell.* **71** (2), 343-353 (1992).
15. Zhang, S. H., Reddick, R. L., Piedrahita, J. A., Maeda, N. Spontaneous hypercholesterolemia and arterial lesions in mice lacking apolipoprotein E. *Science.* **258** (5081), 468-471 (1992).

16. Ishibashi, S. et al. Hypercholesterolemia in low density lipoprotein receptor knockout mice and its reversal by adenovirus-mediated gene delivery. *Journal of Clinical Investigation.* **92** (2), 883-893 (1993).
17. Ishibashi, S., Goldstein, J. L., Brown, M. S., Herz, J., Burns, D. K. Massive xanthomatosis and atherosclerosis in cholesterol-fed low density lipoprotein receptor-negative mice. *Journal of Clinical Investigation.* **93** (5), 1885-1893 (1994).
18. Ketelhuth, D. F., Gistera, A., Johansson, D. K., Hansson, G. K. T cell-based therapies for atherosclerosis. *Current Pharmaceutical Design.* **19** (33), 5850-5858 (2013).
19. Skalen, K. et al. Subendothelial retention of atherogenic lipoproteins in early atherosclerosis. *Nature.* **417** (6890), 750-754 (2002).
20. Boren, J. et al. Identification of the low density lipoprotein receptor-binding site in apolipoprotein B100 and the modulation of its binding activity by the carboxyl terminus in familial defective apo-B100. *Journal of Clinical Investigation.* **101** (5), 1084-1093 (1998).
21. Sanan, D. A. et al. Low density lipoprotein receptor-negative mice expressing human apolipoprotein B-100 develop complex atherosclerotic lesions on a chow diet: no accentuation by apolipoprotein(a). *Proceedings of the National Academy of Sciences of the United States of America.* **95** (8), 4544-4549 (1998).
22. Gistera, A. et al. Vaccination against T-cell epitopes of native ApoB100 reduces vascular inflammation and disease in a humanized mouse model of atherosclerosis. *Journal of Internal Medicine.* (2017).
23. Johnson, J. L., Jackson, C. L. Atherosclerotic plaque rupture in the apolipoprotein E knockout mouse. *Atherosclerosis.* **154** (2), 399-406 (2001).
24. Calara, F. et al. Spontaneous plaque rupture and secondary thrombosis in apolipoprotein E-deficient and LDL receptor-deficient mice. *The Journal of Pathology.* **195** (2), 257-263 (2001).
25. Caligiuri, G., Levy, B., Pernow, J., Thoren, P., Hansson, G. K. Myocardial infarction mediated by endothelin receptor signaling in hypercholesterolemic mice. *Proceedings of the National Academy of Sciences of the United States of America.* **96** (12), 6920-6924 (1999).
26. Daugherty, A. et al. Recommendation on Design, Execution, and Reporting of Animal Atherosclerosis Studies: A Scientific Statement From the American Heart Association. *Arteriosclerosis, Thrombosis, and Vascular Biology.* **37** (9), e131-e157 (2017).
27. Paigen, B., Morrow, A., Holmes, P. A., Mitchell, D., Williams, R. A. Quantitative assessment of atherosclerotic lesions in mice. *Atherosclerosis.* **68** (3), 231-240 (1987).
28. Purcell-Huynh, D. A. et al. Transgenic mice expressing high levels of human apolipoprotein B develop severe atherosclerotic lesions in response to a high-fat diet. *Journal of Clinical Investigation.* **95** (5), 2246-2257 (1995).
29. Nicoletti, A., Kaveri, S., Caligiuri, G., Bariety, J., Hansson, G. K. Immunoglobulin treatment reduces atherosclerosis in apo E knockout mice. *Journal of Clinical Investigation.* **102** (5), 910-918 (1998).
30. Gistera, A., Ketelhuth, D. F. Immunostaining of Lymphocytes in Mouse Atherosclerotic Plaque. *Methods in Molecular Biology.* **1339** 149-159 (2015).
31. Gistera, A. et al. Transforming growth factor-beta signaling in T cells promotes stabilization of atherosclerotic plaques through an interleukin-17-dependent pathway. *Science Translational Medicine.* **5** (196), 196ra100 (2013).
32. Gistera, A. et al. Low-Density Lipoprotein-Reactive T Cells Regulate Plasma Cholesterol Levels and Development of Atherosclerosis in Humanized Hypercholesterolemic Mice. *Circulation.* **138** (22), 2513-2526 (2018).
33. Daugherty, A., Whitman, S. C. Quantification of atherosclerosis in mice. *Methods in Molecular Biology.* **209** 293-309 (2003).
34. Baglione, J., Smith, J. D. Quantitative assay for mouse atherosclerosis in the aortic root. *Methods in Molecular Biology.* **129** 83-95 (2006).
35. Schiller, N. K., Kubo, N., Boisvert, W. A., Curtiss, L. K. Effect of gamma-irradiation and bone marrow transplantation on atherosclerosis in LDL receptor-deficient mice. *Arteriosclerosis, Thrombosis, and Vascular Biology.* **21** (10), 1674-1680 (2001).
36. Naghavi, M. et al. From vulnerable plaque to vulnerable patient: a call for new definitions and risk assessment strategies: Part I. *Circulation.* **108** (14), 1664-1672 (2003).
37. Seijkens, T. T. P. et al. Targeting CD40-Induced TRAF6 Signaling in Macrophages Reduces Atherosclerosis. *Journal of the American College of Cardiology.* **71** (5), 527-542 (2018).